Theoretic approach to ghost imaging in the frequency domain performed by means of a high brilliance coherent monochromatic source

Chiarini, M., Parini, A., Braglia, F., Braglia, L., Braglia, S., et al.

M. Chiarini, A. Parini, F. Braglia, L. Braglia, S. Braglia, S. Farabegoli, A. Artoni, A. Desalvo, G. G. Bentini, "Theoretic approach to ghost imaging in the frequency domain performed by means of a high brilliance coherent monochromatic source," Proc. SPIE 11159, Electro-Optical and Infrared Systems: Technology and Applications XVI, 1115905 (9 October 2019); doi: 10.1117/12.2532307

SPIE.

Event: SPIE Security + Defence, 2019, Strasbourg, France

Theoretic approach to Ghost Imaging in the Frequency Domain performed by means of a high brilliance Coherent Monochromatic Source

M. Chiarini[a]*, A. Parini[a,c], F. Braglia[a], L. Braglia[a], S. Braglia[a], S. Farabegoli[a], A. Artoni[a] , A. Desalvo[b] and G.G. Bentini[a,b]

[a]Prometheus S.r.l., c/o CNR-IMM, Via Gobetti 101, 40129 Bologna, Italy; [b]CNR-IMM, Via Gobetti 101, 40129 Bologna, Italy; [c]Università degli Studi di Ferrara, Via G. Saragat 1, 44122 Ferrara, Italy

ABSTRACT

Ghost imaging is a novel non-conventional technique allowing to generate high resolution images by correlating the intensity of two light beams, neither of which independently contains sufficient information about the spatial distribution and shape of the object. The first demonstration of ghost imaging used light in double photon state, obtained from spontaneous parametric down-conversion. Owing to the entanglement of the source photons, the proposed theory required quantum descriptions for both the optical source and its photo-detection statistics[1]. However, subsequent experimental and theoretical considerations[2,3] demonstrated that ghost imaging can be performed also with thermalized light, utilizing either CCD detector arrays or photon-counting detectors, thus admitting to a semi-classical description, employing classical fields and shot-noise limited detectors. This has generated increasing interest[4-6] in establishing a unifying theory that characterizes the fundamental physics of ghost imaging and defines the boundary between classical and quantum domains. In this view, we exploited recent progress obtained through the application of Fourier Transform Techniques to demonstrate ghost imaging in the frequency domain, in order to measure a continuous spectrum by using a highly brilliant and coherent monochromatic source. In particular, we demonstrate the application of this ghost imaging technique to broadband spectroscopic measurements by means of interaction free photon detection. The experimental apparatus and the collected data are described in a dedicated work[7]. In this paper, we consider the theoretical aspects underlying the proposed Spectroscopic technique. In particular, two alternative theoretical models are presented. In one case, a statistical approach (semi-classical) is applied, where the states of the sampling beam are considered, whereas in the other case a pure quantum treatment is carried on, by describing the interaction of vacuum states generated by photon conversion processes. Both theoretical models, though carried on by means of a complementary formalism, lead to equivalent results and offer a physical interpretation of the collected experimental data. The application of these results offer novel perspectives for remote sensing in low light conditions, or in spectral regions where sensitive detectors are lacking.

Keywords: Ghost Imaging, Spectroscopy, Non Linear Optics, Fourier Transform, Quantum Optics

1. INTRODUCTION

The application of an integrated Asymmetric Non Linear Mach-Zehnder Interferometer (ANLI), provided with an Er:$LiNbO_3$ nonlinear optical element in one arm, allowed to perform interaction-free measurements and to obtain evidence of Ghost Imaging in the frequency domain.

In particular, the obtained experimental results demonstrate the possibility to experimentally determine the structure of the emission lines originated by the nonlinear optical element, placed in one of the arm of the interferometer and interacting with a monochromatic 980nm laser pump source, by only using the information carried by the pump signal itself.

The novelty of this experience resides in the fact that the spectral distribution of the photons converted by Er^{3+} ions was obtained only by using the pump photons, without the need to detect the photons generated by the conversion processes.

The experimental apparatus schematics is reported in Figure 1, whereas the Ghost Imaging results of the Er^{3+} emission lines spectra are reported in Figure 2.

A complete description with extended details of the experimental apparatus, applied to perform the Ghost Imaging experience in the frequency domain, is reported in reference 7.

Electro-Optical and Infrared Systems: Technology and Applications XVI, edited by Duncan L. Hickman, Helge Bürsing,
Proc. of SPIE Vol. 11159, 1115905 · © 2019 SPIE · CCC code: 0277-786X/19/$21 · doi: 10.1117/12.2532307

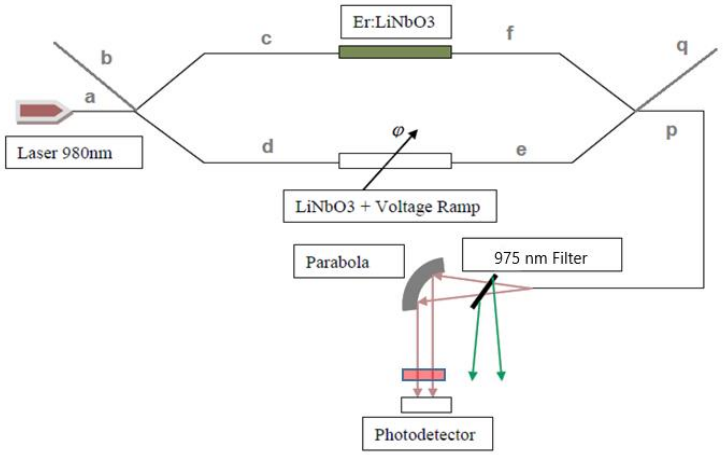

Figure 1. Schematic drawing of the layout used for the present experiment.

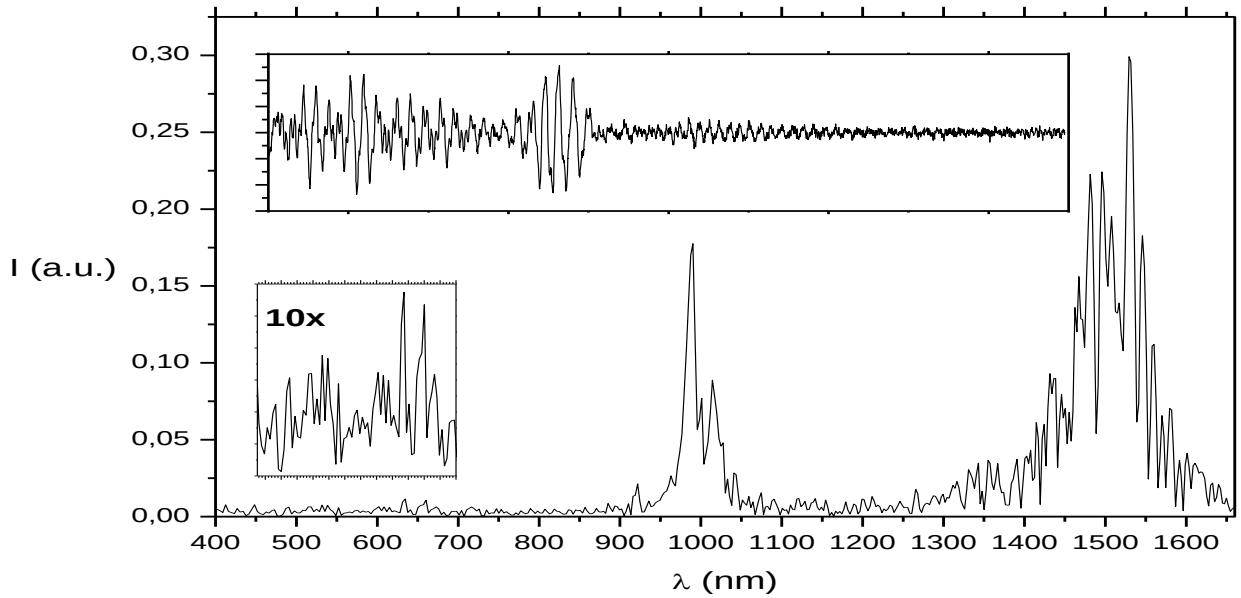

Figure 2. Spectrum obtained by FFT analysis with the experimental set-up of Figure 1, with a Si p-i-n photodetector. The left side inset shows a magnified, (×10), short wavelength part of the spectrum.

Once the 980 nm laser beam was injected into the entry port (a) of the ANLI device, a linear voltage ramp was applied to the undoped arm of the interferometer, to obtain interferograms as a function of time. By Pockels effect, the linear voltage variation gives rise to a corresponding variation of the refractive index generating, in turn, a continuously variating phase shift between the photon states entangled over the two arms of the interferometer. The collected interferograms were analyzed by means of conventional FFT techniques[7], to extract the contained spectral information.

As clearly evidenced by the above-sketched measurement apparatus, the only photons actually detected are those generated by the 980 nm laser pump and non-interacting with the Er^{3+} doped crystal. This is highlighted, particularly considering that the experiment was performed with a wavelength pass band filter (975nm ±25nm) eliminating all up and down

converted photons arriving at the photodetector and then applying a Si p-i-n detector that is 'blind' to I.R. radiation for wavelengths $\lambda \geq 1.1\mu m$.

Nevertheless, despite no photon generated with wavelength different from the one of the pump could reach the detector, we could observe the spectral lines of the Er^{3+} energy levels.

This result also demonstrates that with an ANLI device, we can perform quantitative physical measurements of undetected photons[8,9], hence performing by means of a monochromatic source a Ghost Imaging in the Spectral[10-12] domain of the nonlinear element placed in one arm of the ANLI apparatus.

2. THEORETICAL APPROACH TO THE OBTAINED RESULTS

.

2.1 Quantum Mechanical Interpretation

Considering that the Y junction behaves like a beam splitter, by using the second quantization nomenclature[13,14], we can describe the e.m. field state evolution in the arms *c* and *d* of the interferometer as per the following expression[15-19], namely:

$$|1,0\rangle \rightarrow \frac{1}{\sqrt{2}}[|1,0\rangle + i|0,1\rangle] \tag{1}$$

where, the symbol $|x,y\rangle$ denotes the ordinary tensor product of the Hilbert's space states $|x\rangle \otimes |y\rangle$. The digit 1 symbolizes the presence of one photon whereas the digit 0 symbolizes a vacuum degenerate state. The first symbol refers to the upper arm, (see Figure 1), and the second refers to the lower arm. Following this nomenclature, the symbol $|1,0\rangle$ of Equation (1), means that one photon is propagating in the arm *d* of the ANLI, while a vacuum state is propagating in the arm *c*.

Accordingly, in the above reported notation, the evolution of the different states along the ANLI arms *e* and *f*, (see Figure 1), can be expressed by means of the following expression,

$$(1) \rightarrow 1/\sqrt{2}\,[e^{i\varphi}|1,0\rangle + i(1-\eta(k))|1,0\rangle + ie^{i\varphi}\,\eta(k)|0,0\rangle] \tag{2}$$

In Equation (2) both the phase shift on branch *d* and the nonlinear interaction in branch *c*, are taken into account, where:

$\eta(k)$ is the interaction probability dependent on the *k* values of all the physically admitted transitions determined by the energy levels of the Er^{3+} doped crystal.

In Equation (2), the term $\eta(k)|0,0\rangle$ takes into account that, for each pump photon annihilation with probability $\eta(k)$ in the arm *c*, there is, with the same probability, a corresponding creation of a two mode vacuum state $|0,0\rangle$, propagating in the ANLI.

It is worth noting that in this case we treat the two mode vacuum states $|0,0\rangle$ as actual propagating states (waves) therefore, they are subject to the phase shift applied to the arm *d*.

The term, $e^{i\varphi}\eta(k)|0,0\rangle$ represents the interference of the degenerate vacuum states, produced by annihilation along the doped arm *c*, with the vacuum states entering at the port *b* of the ANLI and propagating in the other arm *d*, entangled with the photon interacting with the Er^{3+} ions. Following these criteria, and maintaining the above reported nomenclature, the variation at the ports *p* and *q* can be written as:

$$(2) \rightarrow \frac{1}{2}[e^{i\varphi}(|1,0\rangle + i|0,1\rangle) + i\big(1-\eta(k)\big)(|0,1\rangle + i|1,0\rangle) + i\eta(k)e^{i\varphi}(|0,0\rangle + i|0,0\rangle)] \tag{3}$$

In particular, the balance of states in Equation (3) takes into account that before reaching the ports *p* and *q*, the states in the arms *e* and *f* are mixed at the Y coupler. Before the Y coupler $|1,0\rangle$ and $|0,1\rangle$ terms represent states of the pump and vacuum propagating in one of the two arms of the ANLI; whereas the $|0,0\rangle$ terms represent the two mode vacuum states propagating in both arms of the ANLI. With some algebra Equation (3) can be developed as follows:

$$(3) \rightarrow \frac{1}{2}[(e^{i\varphi}-1)\big|1,0\rangle + i(e^{i\varphi}+1)|0,1\rangle + \eta(k)\big(\big|1,0\rangle - e^{i\varphi}\big|0,0\rangle\big) - i\eta(k)\big(\big|0,1\rangle + e^{i\varphi}\big|0,0\rangle\big)] \tag{4}$$

The phase variation, $\Delta\varphi$, involves an amplitude variation in the different terms of Equation (4).

Expression (4) is particularly interesting for the physical interpretation of our experimental results. In fact, considering separately the terms of Equation (4), it can be seen that the first two terms

$$\frac{1}{2}[(e^{i\varphi}-1)|1,0\rangle + i(e^{i\varphi}+1)|0,1\rangle] \tag{4a}$$

do not contain the interaction probability $\eta(k)$ and represent the output interferogram of the pump photons that do not interact with the nonlinear doped arm. This output gives rise to a cosine shaped pump interferogram.

The remaining two terms, containing the interaction probability $\eta(k)$,

$$\eta(k)\left(|1,0\rangle - e^{i\varphi}|0,0\rangle\right) - i\eta(k)\left(|0,1\rangle + e^{i\varphi}|0,0\rangle\right) \tag{4b}$$

give rise to an amplitude modulation of the cosine pump interferogram, originating the frequency beats evidenced by our experiments (see Figure 2).

In fact, let us now consider all the states that generate vacuum states e.g. at port q, namely $|u,0\rangle$, with u indicating both 0 and 1, these are given by the following expression

$$\frac{\eta(k)\left(|1,0\rangle - e^{i\varphi}|0,0\rangle\right) - i\eta(k)\left(e^{i\varphi}|0,0\rangle\right)}{2} \tag{4c}$$

The effect of the phase shift on the vacuum states at port q is therefore given by a factor F_q which is function of both k and φ, namely $F_q(\eta(k), \varphi)$. Therefore, thanks to the tensor factorization one can integrate on the states representing the quantum vacuum states arriving at the port q. We can write in place of Equation (4c):

$$F_q(\eta(k), \varphi)\ |u,0\rangle \tag{4d}$$

that is the compact form introduced by Equation (1) of the explicit tensor product
$|u\rangle \otimes F_q(\eta(k), \varphi)\ |0\rangle$.

This expression can be easily rearranged, using De Moivre's and other trigonometric formulas, to explicitly obtain

$$\frac{\eta(k)e^{i\varphi/2}\left(e^{-i\varphi/2}+(1-i)e^{i\varphi/2}\right)}{2}|u,0\rangle = \frac{\eta(k)e^{i\varphi/2}\left(2\cos\left(\frac{\varphi}{2}\right)-i\right)}{2}|u,0\rangle \tag{4e}$$

Therefore, the probability to generate and 'detect' a vacuum state at port q, in terms of modulated interferogram intensity, with respect to the base pump cosine signal, is given by:

$$P_q^{vac} = \langle u,0|u,0\rangle = F_q^*(\eta(k),\varphi)\ F_q(\eta(k),\varphi) = \eta^2(k)\left(1/4 + \cos^2\vartheta\right) \tag{4f}$$

where, $\vartheta = \varphi/2$.

An analogous expression, with $\sin\vartheta$ replacing $\cos\vartheta$, is obtained for port p.

The term represented by Equation (4f), physically adds to the pump cosine signal by introducing the beats that are experimentally observed.

By integrating over all k values, we can obtain the intensity values, I_{out}, registered at ports q and p as a function of ϑ,

$$I_{out,q} = \int_0^\infty \eta^2(k)\cos^2\vartheta\ dk = Const + \int_0^\infty \eta^2(k)\cos(nLk)\ dk \tag{5a}$$

Where:

$$\vartheta = \varphi/2 = kLn/2, \tag{5b}$$

and: n = refractive index, L = length of the electrodes at the arm d.

Likewise, for the port *p* we obtain,

$$I_{out,p} = \int_0^\infty \eta^2(k)\,\sin^2\vartheta\ dk\ = Const - \int_0^\infty \eta^2(k)\cos(nLk)\ dk \tag{5c}$$

It is worth noting that the last term inside the integral of Equations (5), is proportional to the Fourier Transform of the $\eta^2(k)$ term.

As mentioned above, this term physically originates from the vacuum states evolution at the detection port, as a function of the applied phase shift. This means that the beats of the interferogram, allowing to recover the spectral distribution of the excited levels of the doped nonlinear crystal, are generated by the interference of the vacuum states created through the annihilation process of the pump photons. To explain the presence of these spectral lines, it must be considered that the probability $\eta(k)$ of both the pump photons annihilation and the correspondent vacuum states creation, is peaked at the physically admitted transitions of the Er^{3+} dopant.

In practice, within this physical interpretation scheme, our ANLI can be modelled as a two mode device that allows to perform measurements on the *k* axis of the (*k*, δ) phase space describing the System.

Actually, the variables *k* and δ are orthogonal in the phase space and correlated to each other through a Fourier Transform relationship.

In fact, Equation (5a) demonstrates that *k* and δ are conjugate, so it is possible to obtain this result, because the FFT technique exploits the squeezing introduced on the distribution of the *k* variable, by a broadening of the distribution of the conjugated variable δ.

As a consequence, the spectral lines observed in the dimensional space *k* correspond to the levels of the quantum vacuum, generated in the nonlinear crystal.

2.2 Statistical (Semi-classical) Interpretation

Let now focus the attention on the pump statistics, and go back to the first quantization approach[13,14], following the evolution of the pump states as far as the signal travels from the source to the output ports p and q.

Following this approach, one can write[15-19]:

$$|a\rangle \rightarrow \frac{1}{2}\left[e^{i\varphi}(|p>+i|q>) + i\big(1-\eta(k)\big)(|q>+i|p>)\right] \tag{6}$$

Equation (6), expressing the interference pattern, can be written as in the following expression,

$$e^{i\frac{\varphi}{2}}\left(\frac{e^{i\frac{\varphi}{2}}-(1-\eta(k))e^{-i\frac{\varphi}{2}}}{2i}\right)|p> \quad + \quad e^{i\frac{\varphi}{2}}\left(\frac{e^{i\frac{\varphi}{2}}+(1+\eta(k))e^{-i\frac{\varphi}{2}}}{2}\right)|q> \tag{6a}$$

The above expression can be reformulated by means of the usual trigonometric formulas. In particular, considering that

$$e^{i\vartheta} - \alpha e^{-i\vartheta} = (1-i)\,sin(\vartheta+\gamma) + (1+i)\,sin(\vartheta-\gamma)\ ,$$
$$\text{where}\ \ \gamma = tan^{-1}\left[\frac{1+\alpha}{1-\alpha}\right]$$

we observe that, apart from a phase factor $ie^{i\frac{\varphi}{2}}$, Equation (6a) can be written as

$$\left(\frac{(1-i)sin(\vartheta+\gamma)+(1+i)sin(\vartheta-\gamma)}{2i}\right)|p>+$$
$$+\left(\frac{(1-i)sin(\vartheta+\gamma')+(1+i)sin(\vartheta-\gamma')}{2}\right)|q>$$

where

$$\vartheta=\varphi/2,\ \gamma = tan^{-1}\left[\frac{2}{\eta(k)}-1\right]$$
$$\text{and}\ \ \gamma' = tan^{-1}\left[\frac{\eta(k)}{2-\eta(k)}\right]$$

It is worth noting that

$$\gamma + \gamma' = \frac{\pi}{2} \tag{7}$$

Considering that $\eta(k) \ll 1$, one can write

$$\frac{\eta(k)}{2-\eta(k)} \approx \frac{\eta(k)}{2}$$

By using Taylor's expansion for $\tan^{-1}$,

$$tan^{-1}[x] = \sum_{n=1}^{\infty} (-1)^{n+1} \frac{x^n}{n}$$

and, substituting x with $\frac{\eta(k)}{2}$, the γ and γ' parameters can be expressed in Taylor's series, namely,

$$\gamma' = \frac{1}{2}\eta(k) + O(\eta^3(k)) \tag{8a}$$

And then

$$\gamma = \frac{\pi}{2} - \frac{1}{2}\eta(k) + O(\eta^3(k)) \tag{8b}$$

Equation (8a) and (8b) show that one can neglect the rapidly decreasing higher order terms, therefore the weights W_p and W_q of the states |p> and |q>, respectively, can be rewritten as:

$$Wp = \left(\frac{-(1-i)\cos\left(\vartheta - \frac{1}{2}\eta(k)\right) - (1+i)\cos\left(\vartheta + \frac{1}{2}\eta(k)\right)}{2i} \right)$$

And

$$Wq = \left(\frac{(1-i)\sin\left(\vartheta + \frac{1}{2}\eta(k)\right) + (1+i)sin\left(\vartheta - \frac{1}{2}\eta(k)\right)}{2} \right)$$

Then, by computing the probability to detect pump photons at the ANLI output, one finds that

$$P_p \sim <p|p> = \left| \frac{-(1-i)cos\left(\vartheta - \frac{1}{2}\eta(k)\right) - (1+i)cos\left(\vartheta + \frac{1}{2}\eta(k)\right)}{2i} \right|^2$$

$$P_p = cos^2\left(\vartheta - \frac{1}{2}\eta(k)\right) + cos^2\left(\vartheta + \frac{1}{2}\eta(k)\right) \tag{9a}$$

and

$$P_q \sim <q|q> = \left| \frac{(1-i)sin\left(\vartheta + \frac{1}{2}\eta(k)\right) + (1+i)sin\left(\vartheta - \frac{1}{2}\eta(k)\right)}{2} \right|^2$$

$$P_q = sin^2\left(\vartheta - \frac{1}{2}\eta(k)\right) + sin^2\left(\vartheta + \frac{1}{2}\eta(k)\right) \tag{9b}$$

respectively.

Equations (9) can be further manipulated giving the following expressions,

$$P_p \sim sin^2(\vartheta) * sin^2\left(\frac{1}{2}\eta(k)\right) + cos^2(\vartheta) * cos^2\left(\frac{1}{2}\eta(k)\right)$$

$$P_p \sim cos^2(\vartheta) + \frac{1}{4}\eta^2(k) sin^2(\vartheta)$$

and likewise:

$$P_q \sim sin^2(\vartheta) + \frac{1}{4}\eta^2(k) cos^2(\vartheta)$$

Considering e.g. port p, by integrating over all *k*, one obtains the following expression:

$$I_{out} \sim \int_0^\infty \left(\cos^2(\vartheta) + \frac{1}{4}\eta^2(k) \sin^2(\vartheta) \right) \mathrm{dk} = \text{const.} + \int_0^\infty \left(1 - \frac{1}{4}\eta^2(k) \right) \mathbf{cos}(nLk) \ \mathrm{dk} \quad (10)$$

The first term inside the integral of Equation (10) is the output interferogram generated by the pump photons that did not interact with the nonlinear doped element, whereas the last term is the Fourier Transform of the $\eta^2(k)$ term, giving rise to a modulation that sums up to the pump interferogram, yielding to the frequency beats, evidenced by our experiments[7,12].

In particular, the term accounting for the annihilated photons of the pump is matched to the *k* vectors of the photons generated through the interaction with the nonlinear medium due to the energy and momentum conservation laws.

2.3 Comparison between Quantum and Semi-classical Models

Equations (5) and (10), apart from a normalization factor, are identical and demonstrate that starting either from the pump or the degenerate vacuum states perspectives, hence from different physical domains interpretations, one arrives at the same result by means of the Fourier Transform formalism.

3. CONCLUSIONS

The objective of this work was to present a theoretical interpretation of Ghost Imaging in the frequency domain, performed with a high brilliant monochromatic source.

The theoretic model was developed by applying a pure Quantum treatment and alternatively a Semi-classical interpretation, by following Degenerate Vacuum States and Pump States evolution, respectively.

Both treatments lead to the same result, clearly allowing interpreting the observed data in the Fourier Transform formalism.

REFERENCES

[1] Pittman, T. B., Shih, Y. H., Strekalov, D. V. and Sergienko, A. V., "Optical imaging by means of two-photon quantum entanglement," Phys. Rev. A 52, R3429 (1995).

[2] Valencia, A., Scarcelli, G., D'Angelo, M. and Shih, Y.,"Two-Photon Imaging with Thermal Light," Phys. Rev. Lett. 94, 063601 (2005).

[3] Gatti, A., Brambilla, E., Bache, M. and Lugiato, L. A., "Correlated imaging, quantum and classical," Phys. Rev. A 70, 013802 (2004).

[4] Bennink, R. S., Bentley, S. J., Boyd, R. W. and Howell, J. C., "Quantum and Classical Coincidence Imaging," Phys. Rev. Lett. 92, 033601 (2004).

[5] D'Angelo, M., Valencia, A., Rubin, M. H. and Shih, Y., "Resolution of quantum and classical ghost imaging," Phys. Rev. A 72, 013810 (2005)

[6] Erkmen, B. I. and Shapiro, J. H., "Ghost imaging: from quantum to classical to computational," Advances in Optics and Photonics 2(4), 405-450 (2010).

[7] Chiarini, M. et al., "Ghost Imaging in the Frequency Domain with a high brilliance Coherent Monochromatic Source: a novel approach to extend Spectroscopy Sensitivity beyond detectors limits," Proc. SPIE Security & Defense Conference, Strasbourg (2019).

[8] Du Marchie van Voorthuysen, E. H. “Realization of an interaction-free measurement of the presence of an object in a light beam,” Am. J. of Phys. 64(12), 1504-1507 (1996).
[9] Barreto Lemos, G. et al., “Quantum imaging with undetected photons,” Nat. Lett. 512(7565), 409-412 (2014).
[10] Gerry, C. C., Benmoussa, A. and Campos, R. A., “Nonlinear interferometer as a resource for maximally entangled photonic states: Application to interferometry,” Phys. Rev. A 66(1), 013804 1-8 (2002).
[11] Amiot, C., Ryczkowsky, P., Friberg, A.T., Dudley, J.M. and Genty, G., “Supercontinuum spectral-domain ghost imaging,” Opt. Lett. 43(20), 5025-5028 (2018).
[12] Chiarini, M., Bentini, G. G. and Desalvo, A., “Spectroscopy of non-interfering photons through nonlinear integrated optics Mach-Zehnder interferometer,” Proc. SPIE 10230, 1023004-3 (2017).
[13] Lancaster T. and Blundell, S., [Quantum Field Theory for the Gifted Amateurs], Oxford University Press (2012)
[14] Gerry C. C. and Knight, P. L., [Introductory Quantum Optics], Cambridge University Press (2005).
[15] Love, J. D., and Riesen, N., “Single-Few-and Multimode Y-Junctions,” J. of Lightw. Tech. 30(3), 304-309 (2012).
[16] Wilson, J. and Hawkes, J., [Optoelectronics: an Introduction], Prentice Hall Europe (1998).
[17] Zeilinger, A., “General properties of lossless beam splitters in interferometry,” Am. J. Phys 49(9), 882-883 (1981).
[18] Weihs, G. and Zeilinger, A., [Photon statistics at beam splitters: an essential tool in quantum information and teleportation, Coherence and Statistics of Photons and Atom], Perina, J. Editor, Wiley and Wiley (2001).
[19] Kok, P., Lee, H. and Dowling, J. P., “Creation of large-photon-number path entanglement conditioned on photodetection,” Phys. Rev. A 65(5), 052104 1-5 (2002).